ACS APPLIED MATERIALS & INTERFACES

Research Article

www.acsami.org

Vortex-Aligned Fullerene Nanowhiskers as a Scaffold for Orienting Cell Growth

Venkata Krishnan,[†,▽] Yuki Kasuya,[‡] Qingmin Ji,[*,†] Marappan Sathish,[†,○] Lok Kumar Shrestha,[*,†] Shinsuke Ishihara,[§] Kosuke Minami,[†] Hiromi Morita,[∥] Tomohiko Yamazaki,[∥] Nobutaka Hanagata,[*,∥] Kun'ichi Miyazawa,[⊥] Somobrata Acharya,[#] Waka Nakanishi,[†] Jonathan P. Hill,[†] and Katsuhiko Ariga[*,†]

[†]Supermolecules Group, WPI Center for Materials Nanoarchitectonics (MANA), National Institute for Materials Science, 1-1 Namiki, Tsukuba, Ibaraki 305-0044, Japan

[‡]Department of Pure and Applied Chemistry, Tokyo University of Science, 2641 Yamazaki, Noda, Chiba 278-8510, Japan

[§]Functional Geomaterials Group, National Institute for Materials Science (NIMS), 1-1 Namiki, Tsukuba, Ibaraki 305-0044, Japan

[∥]Nanotechnology Innovation Station, National Institute for Materials Science (NIMS), 1-2-1 Sengen, Tsukuba, Ibaraki 305-0047, Japan

[⊥]Fullerene Engineering Group, Exploratory Nanotechnology Research Laboratory, National Institute for Materials Science (NIMS), 1-1 Namiki, Tsukuba, Ibaraki 305-0044, Japan

[#]Centre for Advanced Materials (CAM), Indian Association for the Cultivation of Science (IACS), Jadavpur, Kolkata 700 032, India

Supporting Information

ABSTRACT: A versatile method for the rapid fabrication of aligned fullerene C_{60} nanowhiskers (C_{60}NWs) at the air–water interface is presented. This method is based on the vortex motion of a subphase (water), which directs floating C_{60}NWs to align on the water surface according to the direction of rotational flow. Aligned C_{60}NWs could be transferred onto many different flat substrates, and, in this case, aligned C_{60}NWs on glass substrates were employed as a scaffold for cell culture. Bone forming human osteoblast MG63 cells adhered well to the C_{60}NWs, and their growth was found to be oriented with the axis of the aligned C_{60}NWs. Cells grown on aligned C_{60}NWs were more highly oriented with the axis of alignment than when grown on randomly oriented nanowhiskers. A study of cell proliferation on the C_{60}NWs revealed their low toxicity, indicating their potential for use in biomedical applications.

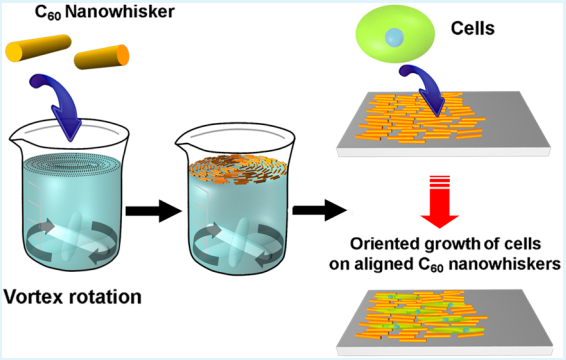

KEYWORDS: *fullerene C_{60} nanowhiskers, vortex-flow-directed assembly, alignment of nanostructures, air–water interface, cell culture*

1. INTRODUCTION

Manipulation of the assembly or alignment of nano- or microstructured materials is essential to exploit fully the potential advantages of their functionalities and to explore their applications in novel electronic, optoelectronic, sensing, or biochip devices.[1−6] Many techniques have been developed for the assembly of nanomaterials,[7−9] with assembly at an air–water interface being an important method for the preparation of various self-assembly patterns.[10−12] The Langmuir–Blodgett (LB) technique facilitates the formation of agglomerated films from molecules or nanostructures by control of lateral compression at the interface surface and circumvents the requirement of complex instrumental installations.[13−16] The driving force for the self-assembly of nanostructures at the air–water interface involves interactions between the capping molecules of the nanostructures and the flow from external slide forces.

Fullerene (C_{60}) is one of the most important carbon-based zero-dimensional nanostructures, and it has been studied extensively for its structural, electronic, and chemical properties.[17−19] Unlike carbon nanotubes (CNTs) and graphene, C_{60} contains 60 carbon atoms arranged in a closed spherical form and exhibits a great diversity from its aggregated morphologies.[20−23] Thus, C_{60} assembles into various one-, two-, and three-dimensional forms upon precipitation from different solvents and solvent mixtures.[24−28] C_{60} nanowhisker (C_{60}NW) is one of the one-dimensional (1D) assembled forms of C_{60} of fibrous morphology which has gained considerable attention owing to its promising applications in solar cells, batteries, fuel cells, sensors, and catalysis, etc.[29−35] Depending on the synthetic conditions, C_{60}NWs with diameters ranging from

Received: June 3, 2015
Accepted: June 26, 2015
Published: June 26, 2015

DOI: 10.1021/acsami.5b04811
ACS Appl. Mater. Interfaces 2015, 7, 15667−15673

100 nm to 1 μm and lengths ranging from 5 to 300 μm can be easily prepared by using the liquid−liquid interfacial precipitation (LLIP) method.[36−38] In contrast to similar needle-like CNTs, the noncovalently assembled structures of C_{60}NWs can be controllably disassembled by application of solvents. Investigations of the biological impact of C_{60}NW also indicate that they may be decomposed to individual C_{60} molecules by macrophage-like cells,[39−41] suggesting their biocompatibility and the future potential of C_{60}NWs for biological applications. Although biological and biomedical applications of fullerenes and CNTs have been explored,[42−45] related studies of C_{60}NWs remain rare despite their huge potential for impact on biological applications so that further exploration is required.

Very recently, we have reported the alignment of C_{60}NWs by using the LB technique and shown that aligned C_{60}NWs can affect cellular phenotype.[46] Here, we propose an innovative method for fabrication technique: vortex-flow-induced alignment strategy, for the rapid and effective alignment of C_{60}NWs at an air−water interface. In this method, the alignment of C_{60}NWs with different packing geometries is induced by vortex flow caused by the mechanical stirring of the medium (Scheme 1a), which differs from typical air−water interfacial assembly methods (Langmuir−Blodgett assembly) where nanostructures are forced to orient in a mutually parallel configuration by compression of barriers. C_{60}NWs orient with the flow of centrifugal rotation at the water surface and could be easily transferred to different flat substrates including paper, mica, glass, boron nitride, and gold. The alignment geometry of C_{60}NWs varies according to the lifting position from the surface: lifting at the region far from the center of rotation yields highly aligned C_{60}NWs in parallel on the substrate while lifting at positions close to the center yields a curved arrangement. Rotation rate also affects the orientation of C_{60}NWs. Compared with conventional alignment methods at an air−water interface, vortex-flow-induced alignment is more effective for alignment of large micrometer-sized structures, especially in the case of fiber-like morphologies. In addition to the provision of linear parallel alignments, this method also enables the curved alignment of C_{60}NWs by controlling the vortex motion. The aligned C_{60}NWs on substrates were used as scaffold for cell cultures (Scheme 1b). It was found that human osteoblast MG63 cells adhere preferentially to the surface of C_{60}NWs (compared to bare glass) and that they tend to grow along the axis of alignment of the C_{60}NWs. Furthermore, cell proliferation studies revealed the low-toxicity nature of C_{60}NWs revealing aligned C_{60}NWs as an excellent new potential candidate for biological and biomedical applications.

Scheme 1. Schemes for (a) the Alignment C_{60}NWs at an Air−Water Interface by Vortex Flow and (b) Aligned C_{60}NWs as Scaffold for Directing Cell Growth

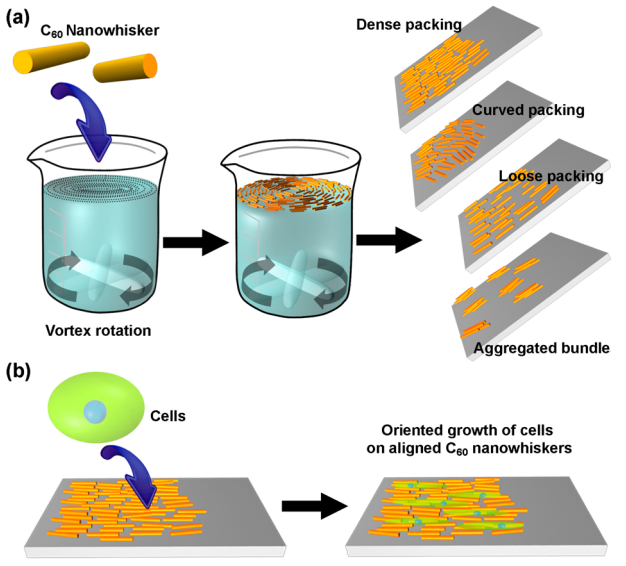

2. EXPERIMENTAL SECTION

2.1. Materials. Pristine fullerene C_{60} powder with purity > 99.5% was purchased from Materials Technologies Research, Ltd. (Cleveland, OH, USA). Toluene (Tol) and isopropyl alcohol (IPA) with purity > 99% were purchased from the Wako Chemical Corp., Japan. All chemicals were used as received.

2.2. Preparation and Purification of C_{60}NW. C_{60}NWs were prepared using the liquid−liquid interfacial precipitation (LLIP) method.[36,47] A saturated solution of C_{60} in toluene was prepared by treating an excess of pristine C_{60} powder (80 mg) with 25 mL of toluene. Undissolved C_{60} was removed by filtration. In a typical preparation process of C_{60}NW, a portion of the saturated solution of C_{60} in toluene (4 mL) was placed in a clean, dry glass vial (20 mL) and cooled to 4 °C in a temperature-controlled incubator for 2 h. IPA (4 mL), which had also been precooled at 4 °C for 2 h, was then layered slowly on top of the saturated C_{60} solution in toluene, and the resulting mixture was stored at 4 °C for 1−4 days. The mixture/solution turned brownish due to the formation of C_{60}NWs. The resulting C_{60}NWs were first purified by centrifugation for 2 min at 4000 rpm, whereby C_{60}NWs precipitated, and the supernatant containing unreacted C_{60} was discarded. The C_{60}NWs were then washed once with IPA and again centrifuged for 2 min at 4000 rpm. The thus purified C_{60}NWs were then resuspended in IPA (3 mg/mL) and stored at room temperature prior to use.

2.3. Alignment of C_{60}NWs. The suspension of C_{60}NWs was added dropwise (at a rate of about 10 drops/min) to the surface of ultrapure water (90 mL, with constant stirring at 150 rpm) contained in a 100 mL beaker. A magnetic stirrer bar of length that was almost the interior diameter of the beaker (~5 cm) was used. The process was performed at 25 °C. Addition of the C_{60}NW suspension was continued until the entire surface of the water was covered by a uniform thin layer of C_{60}NWs (as judged by the naked eye). For a 100 mL beaker, the quantity of added C_{60}NW suspension was optimized at 0.9 mL. After formation of the thin film, stirring was stopped and the system was left undisturbed for 5 min to allow evaporation of the IPA. For the deposition of aligned C_{60}NWs on substrates, glass microscope slides or silicon wafer was cut into pieces (2 cm × 1 cm) and consecutively cleaned with acetone, ethanol, and water and then dried. The transfer of aligned C_{60}NWs film onto the substrates was performed by hand by using a gentle scooping action with the required substrate held in tweezers. A maximum of four substrates could be coated with C_{60}NWs film from one spreading procedure.

2.4. Characterizations. Scanning electron micrographs (SEMs) were obtained using a Hitachi S-4800 FE-SEM instrument. Samples for SEMs were prepared on a Si wafer and dried under reduced pressure prior to measurements. Optical microscopic images were obtained using an Olympus MP5Mc/OL microscope. Raman spectra were obtained using a JASCO NRS-3100 laser Raman spectrometer operating at a wavelength of 532 nm with the power level set to 1.0 mW. Powder X-ray diffraction (XRD) patterns were measured on a Rigaku RINT 1200 diffractometer using Ni-filtered Cu K_α radiation (λ = 1.5418 Å) with an operating voltage of 40 kV and beam current of 30 mA.

2.5. Image Analysis. Image analysis software, ImageJ 1.44p from NIH (National Institute of Health, Bethesda, MD, USA),[48] was used for the detailed analysis of SEM images in order to quantitatively evaluate the alignment distribution and the angle of orientation. The alignment distribution of C_{60}NW was determined directly by

DOI: 10.1021/acsami.5b04811
ACS Appl. Mater. Interfaces 2015, 7, 15667−15673

measuring the angle of orientation of C_{60}NW with respect to the surface normal of the SEM images. For cell culture samples, the angle of orientation of cells and the angle of orientation of the adjoining C_{60}NWs were determined directly from the SEM images and plotted as a function of each other for random and aligned C_{60}NWs.

2.6. Cell Culture. Human osteoblast-like MG63 cells (Riken, Wako, Japan) were cultured in Dulbecco's modified Eagle's medium (DMEM) supplemented with 10% fetal bovine serum (FBS), 1% penicillin/streptomycin at 37 °C in a humidified atmosphere with 5% CO_2. The medium was changed several times each week. The cells were trypsinized and resuspended in fresh media.

2.7. Adhesion and Proliferation of MG63 Cells on the Substrates. Random or aligned C_{60}NWs on slide glass were placed into a 24-well plate (Thermo Fisher Scientific Inc., Waltham, MA, USA), and MG63 cells were seeded at a density of 1.0×10^4 cells cm^{-2} with the culture medium. Cells were cultured at 37 °C in a humidified atmosphere containing 5% CO_2. The number of MG63 cells for 4, 24, and 48 h was determined by water-soluble tetrazolium salt (WST) assay using cell counting kit-8 (Dojindo, Kumamoto, Japan).

Cellular morphology was investigated by examining the cytoskeleton fluorescently stained with fluorescein isothiocyanate (FITC)-conjugated phalloidin.

3. RESULTS AND DISCUSSION

C_{60}NWs from the LLIP Method. C_{60}NWs were produced at an interface formed between IPA and a saturated solution of C_{60} in toluene (Tol) using the LLIP method. To avoid the formation of inhomogeneous structures (formed due to fast growth), C_{60}NWs were produced at 4 °C. The resulting C_{60}NWs formed a stable dispersion in IPA without precipitation for at least 3 months at room temperature (Figure 1a). Figure 1 shows a photographic image of C_{60}NWs

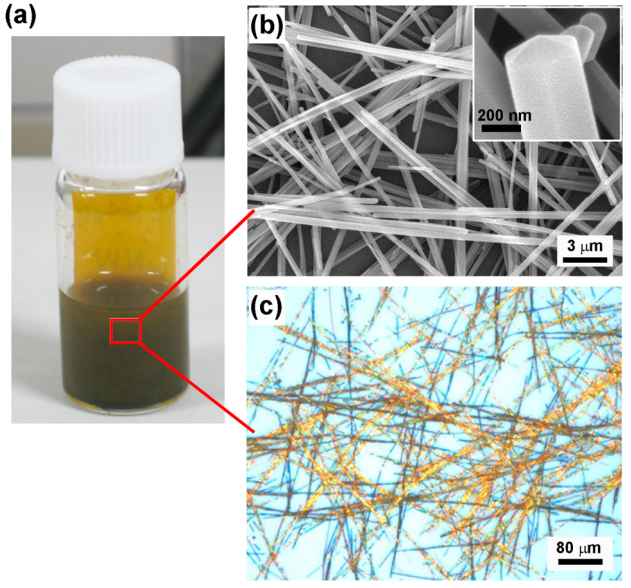

Figure 1. (a) Photograph of C_{60}NW dispersion in IPA, (b) SEM, and (c) optical microscopic images of randomly arranged C_{60}NW. Inset of panel b shows a high magnification SEM image of an individual rod illustrating the faceted structure.

dispersed in IPA, a corresponding SEM image (Figure 1b), and an optical microscopic image of the rod-like nanowhiskers (Figure 1c). Average diameters and lengths of the C_{60}NWs are ca. ~500 nm and ~250 μm, respectively. They possess smooth surfaces along their entire lengths with clear facets (see inset of Figure 1b). The aspect ratio of C_{60}NWs could be flexibly controlled simply by altering the volume of IPA and C_{60} solution in Tol and their mixing ratios. For example, C_{60}NWs obtained by decreasing the total solvent volume from 8 mL (IPA:Tol, 4:4) to 4 mL (IPA:Tol, 2:2) exhibited larger average diameters ca. ~800 nm and shorter lengths ca. ~20 μm (Supporting Information Figure S1). On the other hand, C_{60}NWs grown at a mixing ratio of IPA:Tol = 6:2 showed average diameters and lengths around 300 nm and 50 μm, respectively. Note that the aspect ratio of the C_{60}NWs influences the alignment of C_{60}NWs at an air–water interface (see later for a discussion of this point).

The C_{60}NWs prepared here exhibited spectroscopic features similar to those of pristine C_{60} (Figure 2). The "pentagonal

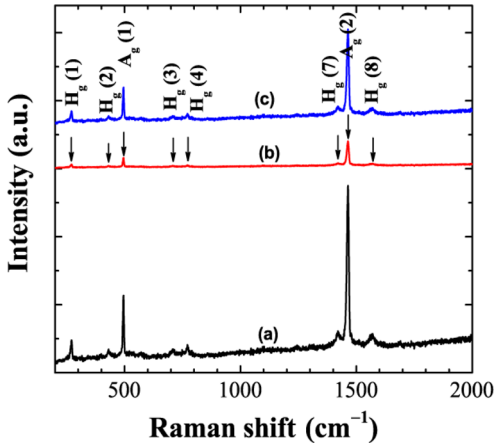

Figure 2. Raman spectra of (a) pristine C_{60}, (b) C_{60}NWs, and (c) C_{60}NWs aligned by vortex-flow method.

pinch" mode or $A_g(2)$ band that appears around 1468 cm^{-1} in the Raman spectrum of C_{60} is regarded as an analytical probe of the structural and electronic properties of C_{60}. The $A_g(2)$ bands of C_{60}NWs and pristine C_{60} are essentially identical demonstrating that these C_{60}NWs contain C_{60} in its original monomeric form; i.e., C_{60} molecules in the C_{60}NWs interact through weak van der Waals forces. The crystalline structure of the obtained C_{60}NWs was investigated by XRD (Supporting Information Figure S2) revealing diffraction peaks at 2θ = 10.7°, 17.7°, 20.6°, and 21.6° (weak) for C_{60}NWs, which are assigned to the (111), (022), (113), and (222) planes of a face-centered cubic (FCC) structure with lattice constant of a = 1.420 nm, comparable to the lattice constant of pristine C_{60} ca. 1.418 nm demonstrating that the prepared C_{60}NW crystals have a high purity.[49,50]

Vortex-Flow-Directed Alignment of C_{60}NWs. Alignment of C_{60}NWs at the air–water interface was performed in glass beakers. The water subphase was stirred with a constant rate (150 rpm) during the addition of the C_{60}NW suspension in IPA. Under this mechanical rotary stirring, a spiral flow at the bottom of the beaker generates vortex motion at the surface; i.e., the water surface is no longer flat but is depressed at the center and rises near the walls of the beaker (Supporting Information Figure S3). The suspension of C_{60}NWs was carefully dropped at the center of the water surface. Due to their highly hydrophobic nature (contact angle of C_{60}NW is ca. ~134°), C_{60}NWs float on the water surface. Furthermore, the velocity gradient of water motion and the centrifugal rotation spread the C_{60}NWs on the surface preventing their random aggregation (Supporting Information Figure S4). Stirring was stopped when an almost homogeneous distribution of the

DOI: 10.1021/acsami.5b04811
ACS Appl. Mater. Interfaces 2015, 7, 15667–15673

C_{60}NWs could be observed (by eye) at the water surface. The influence of stirring rate on the alignment of C_{60}NWs was also investigated. It was found that 150 rpm is an appropriate stirring speed for the alignment of C_{60}NWs having lengths and diameters of ~250 μm and 500 nm, respectively. At slower stirring rates (<150 rpm), where the vortex motion at the surface is not obvious and the surface of the water appears almost flat (Supporting Information Figure S3b,c), C_{60}NWs are poorly aligned with large gaps among the C_{60}NWs (Supporting Information Figure S5a,b). On the other hand, at higher stirring rates (>150 rpm), the surface of the water adopts a deep parabolic shape due to a stronger centripetal force and downward water flow peripheral to the vortex center may increase (Supporting Information Figure S3e,f) causing aggregation of the C_{60}NWs into bundles. Under this condition, alignment is even more severely disrupted than for the lower stirring rates (Supporting Information Figure S5c).

Considering the shear force between the water and the floating C_{60}NWs, the dimensions of the C_{60}NWs, especially the length, may affect alignment. Therefore, we have also investigated the influence of C_{60}NW length on their alignment at a constant stirring speed of 150 rpm. Average diameters of the C_{60}NWs were essentially invariant at ~500 nm. We found that, when compared to the longer C_{60}NWs (250 μm), the shorter C_{60}NWs (~20 μm) were loosely aligned with many void spaces (Supporting Information Figure S6a,b). With further decrease in the lengths of C_{60}NWs (~5 μm), unidirectional alignment could not be achieved (Supporting Information Figure S6c), although C_{60}NWs were compressed into dense aggregates. The lower shear force between short C_{60}NWs and water may weaken the compression of C_{60}NWs along the current caused by the vortex rotation resulting in the loose packing and a large angular deviation of the aligned C_{60}NWs.

When stirring is stopped and the water surface attains a flat surface, a concurrent shrinkage of the surface area further compresses the aligned C_{60}NWs, promoting the formation of a more compact layer of C_{60}NWs. The floating array of C_{60}NWs was transferred onto flat substrates by pulling and lifting from the water surface. Different substrates including Si, glass, BN, gold, and filter paper could be used to collect the aligned C_{60}NWs (Supporting Information Figure S7). Note that the location of the lifting position at the surface results in different packing structures of the aligned C_{60}NWs due to the gradient of radial velocities from the vortex center to the periphery.

Parts a and c of Figure 3 show SEM images of C_{60}NWs arrays lifted at regions close to the edge of the beaker. Here, a closely packed formation of C_{60}NWs with a few partially overlapped bundles can be seen. The C_{60}NWs are arranged in parallel over areas of several hundred square micrometers on the substrate. C_{60}NWs arrays lifted from the center of the beaker exhibit curved packing of the bundles of C_{60}NWs (Figure 3b,d), which is anticipated to be induced by larger vorticity at the center of stirring.

The density and packing of the aligned C_{60}NWs differ depending on the affinity of the lifting substrate for water. For instance, compared to hydrophobic Si wafer (contact angle ~ 65°), looser packing of C_{60}NWs with wider voids was observed on hydrophilic glass slide (contact angle ~ 45°) and mica (contact angle ~ 23°) substrates (Supporting Information Figure S8). Furthermore, the alignments of C_{60}NWs are nondirectional indicating that the surface hydrophobicity/or

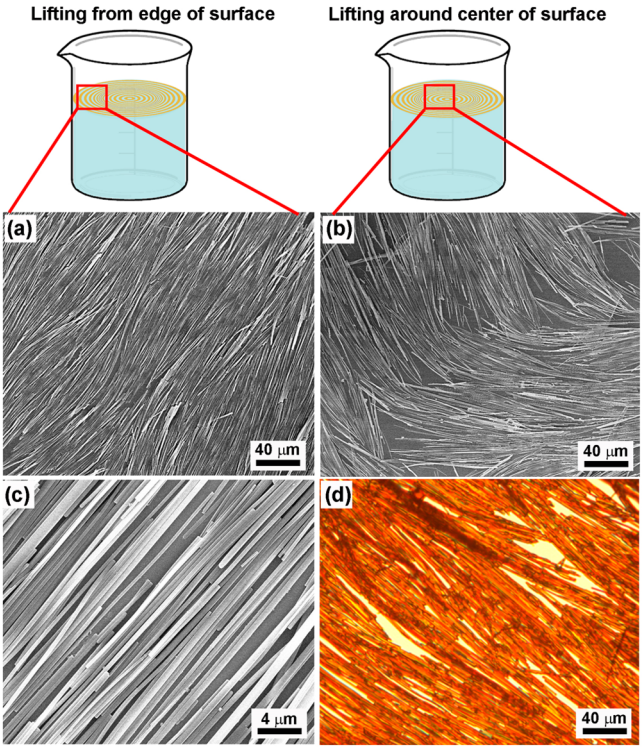

Figure 3. (a, c) SEM images of aligned C_{60}NWs on Si substrate lifted from the surface near the edge of the beaker wall, (b) SEM image of aligned C_{60}NWs lifted from the vortex rotation center, and (d) optical microscopic image of aligned C_{60}NWs.

hydrophilicity of the substrate plays a key role on the packing density and orientation of the resulting C_{60}NWs arrays.

The aligned C_{60}NWs remained strongly adhered to the substrates even after comprehensive drying under reduced pressure. Also, the aligned C_{60}NWs did not peel off from the Si or glass substrates even after immersion in water or ethanol for several days. Note that the alignment of C_{60}NWs at the water surface and their transfer to a substrate does not influence the molecular structure of C_{60}NWs.

For comparison, alignment of C_{60}NWs has also been performed by using the Langmuir–Blodgett (LB) approach. C_{60}NWs spread on a water surface were compressed at surface pressures of 5 or 25 mN/m and the packed structures were transferred onto a Si substrate (Supporting Information Figure S9). At both these surface pressures, C_{60}NWs were not well aligned on the substrate. The compressive force applied in the LB method may not be sufficiently strong to form ordered structures from high aspect ratio morphology C_{60}NWs, leading to poor or no alignment of C_{60}NWs along their long axes. This observation demonstrates that the vortex-flow method is advantageous over LB compression for the effective alignment of microsized 1D structures.

Aligned C_{60}NWs as Scaffold for Cell Culture. Aligned C_{60}NWs on slide glass were used without any further surface modification as a scaffold for directing cell growth. These arrays of C_{60}NWs may form rough micro- and/or macrosized surface features that might act as grooves for growth of cells. When human osteoblast cell line MG63 was cultured on the aligned C_{60}NWs, the cells preferentially adhered to the surfaces of C_{60}NWs and tended to grow along the alignment axis of the C_{60}NWs arrays (Figure 4).

DOI: 10.1021/acsami.5b04811
ACS Appl. Mater. Interfaces 2015, 7, 15667–15673

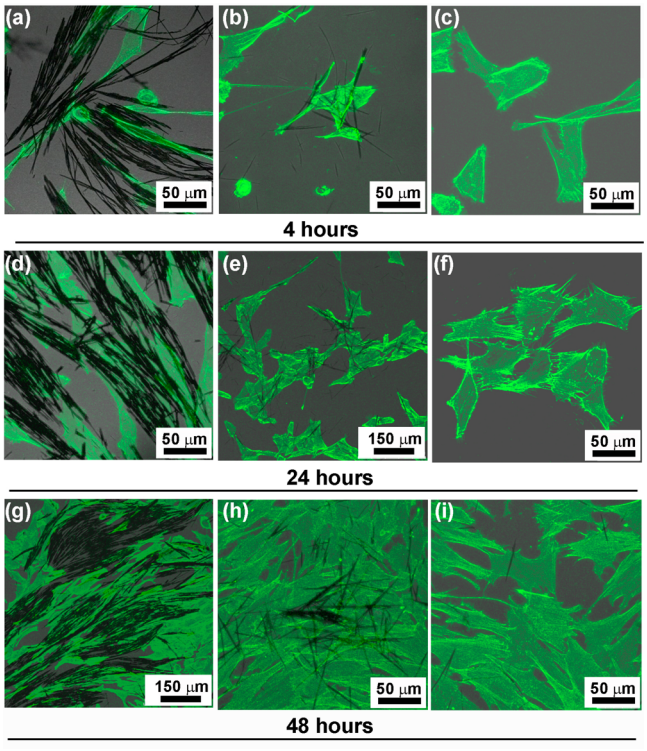

Figure 4. Fluorescence microscopy images illustrating the growth of human osteoblast cell line MG63 on (a, d, g) aligned C_{60}NWs, (b, e, h) random C_{60}NWs, and (c, f, i) slide glass after inoculation for 4, 24, and 48 h, respectively.

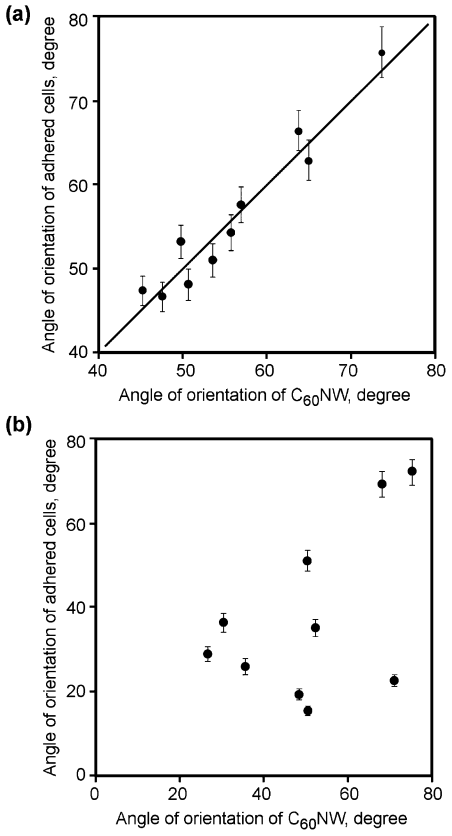

Figure 5. Angle of orientation of cells as a function of angle of orientation of C_{60}NW for cells cultured for (a) 24 h on aligned C_{60}NW and (b) random C_{60}NWs.

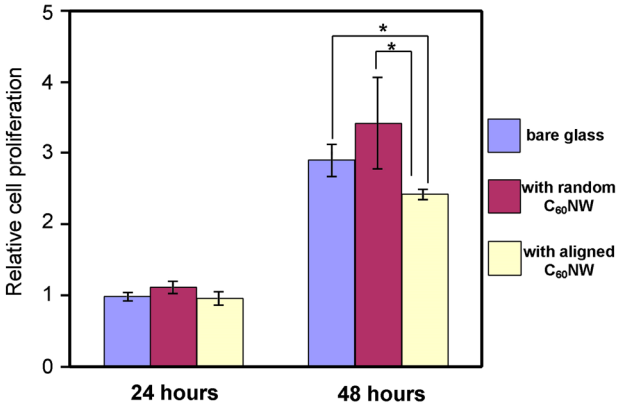

Figure 6. Cell proliferation as a function of time illustrating the growth of human osteoblast cell line MG63 on random and aligned C_{60}NWs along with glass. Asterisks (*) indicate $P < 0.05$ versus bare glass.

From an investigation of the cells grown on low-density aligned C_{60}NWs with, we found that more cells bound to the C_{60}NWs rather than the glass surface irrespective of the hydrophobic nature of C_{60}NWs. It has been suggested that the π-electronic systems of carbon clusters may aid in the adsorption of extracellular matrix, which facilitates cell adhesion.[46,51] Surface roughness may also play an important role for the adhesion of cells.[52,53]

Further comparison with bare slide glass and random C_{60}NWs over longer culture times indicate that the aligned C_{60}NWs influence strongly the shape of the growing cells. Cells grown on random C_{60}NWs or on bare glass tend to attain a round morphology, while an elongated or rod-like growth shape coinciding with the alignment axis of C_{60}NWs was observed for the case of the aligned C_{60}NW arrays (Figure 4 and Supporting Information Figure S10). The orientation of cell growth along the axis of alignment for the aligned C_{60}NWs is also illustrated by the linear correlation between the angle of orientation of C_{60}NWs and the cultured cells (Figure 5a). Conversely, cells grew in all directions for random C_{60}NWs, and no correlation could be detected between their angles of orientation (Figure 5b).

Cell proliferation on aligned C_{60}NWs was assessed relative to bare slide glass and random C_{60}NWs as controls. Equal numbers of cells were plated on the substrates and cultured for 24 and 48 h. As shown in Figure 6, there was an approximately 3-fold increase in the number of viable cells during the subsequent 24 h (24–48 h), implying the low toxicity of the C_{60}NWs as a scaffold for the cell growth. The proliferation value for aligned C_{60}NWs was slightly lower than that for bare slide glass or random C_{60}NWs. Considering the growth of cells in all directions for the cases of bare slide glass and random C_{60}NWs, the aligned C_{60}NWs confine cell growth predominantly along their long axis direction, but may weakly restrain cell growth. This suppression of cell growth on the aligned C_{60}NWs should have no inhibitory effect on differentiation or the cell cycle.[46]

These results reveal that aligned C_{60}NWs are a potential substrate for the adhesion, growth, and maturation of human osteoblast cell line MG63, being comparable to standard cell culture materials such as tissue culture polystyrene. The structured surface of C_{60}NW enhances the adsorption of cell adhesion-mediating extracellular matrix (ECM) molecules, such as vitronectin, fibronectin, and collagen, either provided by the

DOI: 10.1021/acsami.5b04811
ACS Appl. Mater. Interfaces 2015, 7, 15667–15673

serum of the cell culture medium or synthesized by the cells. The cells interact with the substrate's topological structures through a phenomenon known as contact guidance, which is characterized by the response of the cells to the structure at the micrometer and sub-micrometer scale.[54,55] The mechanism of oriented cell growth on aligned C_{60}NWs can be attributed to the spatially controlled preferential adhesion and active cell−substrate interaction followed by signal transduction inside the cells.[56,57] Thus, the aligned C_{60}NWs promote cell colonization in the direction of their alignment.

4. CONCLUSIONS

We have demonstrated a new method of creating aligned C_{60}NWs at the air−water interface. The process is based on spreading of a C_{60}NWs dispersion over a water surface and directing the alignment of C_{60}NWs by vortex flow of water. The aligned C_{60}NWs could be easily transferred onto any flat substrate irrespective of material. Compared to the other fabrication techniques such as drop-casting, spin-coating, LB, and layer-by-layer (LbL) methods, this method offers the freedom of ease of implementation without much concern for too-dense aggregation (drop-casting), low surface coverage (spin-coating), relatively larger sample amount required (LB method), and immobilization forces on substrates (LbL method). The packing geometry and density of the C_{60}NW arrays could easily be controlled by varying the quantity of C_{60}NWs, stirring rate, lifting position, and surface hydrophobicity of the substrate.

The aligned C_{60}NWs on substrates functioned as a remarkable substrate for the cell culture. Human osteoblast MG63 cells adhered well and underwent oriented growth along the aligned C_{60}NWs. We believe that, after optimization of the alignment process, other kinds of nanostructures or microstructures (2D or 3D) can be formed into highly organized and well-defined 2D architectures.

■ ASSOCIATED CONTENT

Supporting Information

Further experimental information including XRD results, a variety of optical images, SEM images, and photographs of different vortex rotation rates, water surface under vortex rotation, and aligned C_{60}NWs deposited on substrates. The Supporting Information is available free of charge on the ACS Publications website at DOI: 10.1021/acsami.5b04811.

■ AUTHOR INFORMATION

Corresponding Authors

*(Q.J.) E-mail: JI.Qingmin@nims.go.jp.
*(L.K.S.) E-mail: SHRESTHA.Lokkumar@nims.go.jp.
*(N.H.) E-mail: HANAGATA.Nobutaka@nims.go.jp.
*(K.A.) E-mail: ARIGA.Katsuhiko@nims.go.jp.

Present Addresses

[∇]School of Basic Sciences, Indian Institute of Technology Mandi, Mandi 175-001, Himachal Pradesh, India.
[○]Functional Materials Division, CSIR-Central Electrochemical Research Institute, Karaikudi 630 006, India.

Notes

The authors declare no competing financial interest.

■ ACKNOWLEDGMENTS

This research was supported by World Premier International Research Center Initiative (WPI Initiative) on Materials Nanoarchitectonics, from MEXT Japan, and the CREST program of Japan Science and Technology Agency (JST), Japan.

■ REFERENCES

(1) Ariga, K.; Ji, Q.; Nakanishi, W.; Hill, J. P. Thin Film Nanoarchitectonics. *J. Inorg. Organomet. Polym. Mater.* **2015**, *25*, 466−479.
(2) Ariga, K.; Yamauchi, Y.; Ji, Q.; Yonamine, Y.; Hill, J. P. Mesoporous Sensor Nanoarchitectonics. *APL Mater.* **2014**, *2*, 030701.
(3) Ariga, K.; Kawakami, K.; Ebara, M.; Kotsuchibashi, Y.; Ji, Q.; Hill, J. P. Bioinspired Nanoarchitectonics as Emerging Drug Delivery Systems. *New J. Chem.* **2014**, *38*, 5149−5163.
(4) Kim, F. S.; Ren, G. Q.; Jenekhe, S. A. One-Dimensional Nanostructures of π-Conjugated Molecular Systems: Assembly, Properties, and Applications from Photovoltaics, Sensors, and Nanophotonics to Nanoelectronics. *Chem. Mater.* **2011**, *23*, 682−732.
(5) Sun, T. L.; Qing, G. Y.; Su, B. L.; Jiang, L. Functional Biointerface Materials Inspired from Nature. *Chem. Soc. Rev.* **2011**, *40*, 2909−2921.
(6) Rorvik, P. M.; Grande, T.; Einarsrud, M. A. One-Dimensional Nanostructures of Ferroelectric Perovskites. *Adv. Mater. (Weinheim, Ger.)* **2011**, *23*, 4007−4034.
(7) Sakakibara, K.; Hill, J. P.; Ariga, K. Thin-Film-Based Nanoarchitectures for Soft Matter: Controlled Assemblies into Two-Dimensional Worlds. *Small* **2011**, *7*, 1288−1308.
(8) Grinthal, A.; Kang, S. H.; Epstein, A. K.; Aizenberg, M.; Khan, M.; Aizenberg, J. Steering Nanofibers: An Integrative Approach to Bio-Inspired Fiber Fabrication and Assembly. *Nano Today* **2012**, *7*, 35−52.
(9) Kim, H. N.; Jiao, A.; Hwang, N. S.; Kim, M. S.; Kang, D. H.; Kim, D. H.; Suh, K. Y. Nanotopography-Guided Tissue Engineering and Regenerative Medicine. *Adv. Drug Delivery Rev.* **2013**, *65*, 536−558.
(10) Matharu, Z.; Bandodkar, A. J.; Gupta, V.; Malhotra, B. D. Fundamentals and Application of Ordered Molecular Assemblies to Affinity Biosensing. *Chem. Soc. Rev.* **2012**, *41*, 1363−1402.
(11) Sakakibara, K.; Chithra, P.; Das, B.; Mori, T.; Akada, M.; Labuta, J.; Tsuruoka, T.; Maji, S.; Furumi, S.; Shrestha, L. K.; Hill, J. P.; Acharya, S.; Ariga, K.; Ajayaghosh, A. Aligned 1-D Nanorods of a π-Gelator Exhibit Molecular Orientation and Excitation Energy Transport Different from Entangled Fiber Networks. *J. Am. Chem. Soc.* **2014**, *136*, 8548−8551.
(12) Tang, P. Q.; Hao, J. C. Macroporous Honeycomb Films of Surfactant-Encapsulated Polyoxometalates at Air/Water Interface and Their Electrochemical Properties. *Adv. Colloid Interface Sci.* **2010**, *161*, 163−170.
(13) Ariga, K.; Mori, T.; Hill, J. P. Interfacial Nanoarchitectonics: Lateral and Vertical, Static and Dynamic. *Langmuir* **2013**, *29*, 8459−8471.
(14) Tao, A. R.; Huang, J. X.; Yang, P. D. Langmuir−Blodgettry of Nanocrystals and Nanowires. *Acc. Chem. Res.* **2008**, *41*, 1662−1673.
(15) Zasadzinski, J. A.; Viswanathan, R.; Madsen, L.; Garnaes, J.; Schwartz, D. K. Langmuir-Blodgett Films. *Science* **1994**, *263*, 1726−1733.
(16) Acharya, S.; Panda, A. B.; Belman, N.; Efrima, S.; Golan, Y. A Semiconductor-Nanowire Assembly of Ultrahigh Junction Density by the Langmuir−Blodgett Technique. *Adv. Mater. (Weinheim, Ger.)* **2006**, *18*, 210−213.
(17) Kroto, H. W.; Heath, J. R.; O'Brien, S. C.; Curl, R. F.; Smalley, R. E. C_{60}: Buckminsterfullerene. *Nature* **1985**, *318*, 162−163.
(18) Kratshcmer, W.; Lamb, L. D.; Fostiropoulos, K.; Huffman, D. R. Solid C_{60}: A New Form of Carbon. *Nature* **1990**, *347*, 354−358.
(19) Bonifazi, D.; Enger, O.; Diederich, F. Supramolecular [60]-Fullerene Chemistry on Surfaces. *Chem. Soc. Rev.* **2007**, *36*, 390−414.
(20) Guldi, D. M.; Zerbetto, F.; Georgakilas, V.; Prato, M. Ordering Fullerene Materials at Nanometer Dimensions. *Acc. Chem. Res.* **2005**, *38*, 38−43.
(21) Cassell, A. M.; Asplund, C. L.; Tour, J. M. Self-Assembling Supramolecular Nanostructures from a C(60) Derivative: Nanorods and Vesicles. *Angew. Chem., Int. Ed.* **1999**, *38*, 2403−2405.

DOI: 10.1021/acsami.5b04811
ACS Appl. Mater. Interfaces 2015, 7, 15667−15673

(22) Nakanishi, T.; Ariga, K.; Michinobu, T.; Yoshida, K.; Takahashi, H.; Teranishi, T.; Möhwald, H.; Kurth, D. G. Flower-Shaped Supramolecular Assemblies: Hierarchical Organization of a Fullerene Bearing Long Aliphatic Chains. *Small* **2007**, *3*, 2019−2023.
(23) Zhang, X. Y.; Hsu, C. H.; Ren, X. K.; Gu, Y.; Song, B.; Sun, H. J.; Yang, S.; Chen, E.; Tu, Y. F.; Li, X. H.; Yang, X. M.; Li, Y. W.; Zhu, X. L. Supramolecular [60]Fullerene Liquid Crystals Formed By Self-Organized Two-Dimensional Crystals. *Angew. Chem., Int. Ed.* **2015**, *54*, 114−117.
(24) Nakanishi, T.; Schmitt, W.; Michinobu, T.; Kurth, D. G.; Ariga, K. Hierarchical Supramolecular Fullerene Architectures with Controlled Dimensionality. *Chem. Commun.* **2005**, *48*, 5982−5984.
(25) Sathish, M.; Miyazawa, K. Size-Tunable Hexagonal Fullerene (C_{60}) Nanosheets at the Liquid−Liquid Interface. *J. Am. Chem. Soc.* **2007**, *129*, 13816−13817.
(26) Wei, L.; Lei, Y.; Fu, H.; Yao, J. Fullerene Hollow Microspheres Prepared by Bubble-Templates as Sensitive and Selective Electrocatalytic Sensor for Biomolecules. *ACS Appl. Mater. Interfaces* **2012**, *4*, 1594−1600.
(27) Wakahara, T.; Sathish, M.; Miyazawa, K.; Hu, C. P.; Tateyama, Y.; Nemoto, Y.; Sasaki, T.; Ito, O. Preparation and Optical Properties of Fullerene/Ferrocene Hybrid Hexagonal Nanosheets and Large-Scale Production of Fullerene Hexagonal Nanosheets. *J. Am. Chem. Soc.* **2009**, *131*, 9940−9944.
(28) Shrestha, L. K.; Ji, Q. M.; Mori, T.; Miyazawa, K.; Yamauchi, Y.; Hill, J. P.; Ariga, K. Fullerene Nanoarchitectonics: From Zero to Higher Dimensions. *Chem. - Asian J.* **2013**, *8*, 1662−1679.
(29) Somani, P. R.; Somani, S. P.; Umeno, M. Toward Organic Thick Film Solar Cells: Three Dimensional Bulk Heterojunction Organic Thick Film Solar Cell Using Fullerene Single Crystal Nanorods. *Appl. Phys. Lett.* **2007**, *91*, 173503.
(30) Ji, H.-X.; Hu, J. S.; Wan, L. J.; Tang, Q. X.; Hu, W. P. Controllable Crystalline Structure of Fullerene Nanorods and Transport Properties of an Individual Nanorod. *J. Mater. Chem.* **2008**, *18*, 328−332.
(31) Shrestha, L. K.; Shrestha, R. G.; Yamauchi, Y.; Hill, J. P.; Nishimura, T.; Miyazawa, K.; Kawai, T.; Okada, S.; Wakabayashi, K.; Ariga, K. Nanoporous Carbon Tubes from Fullerene Crystals as the π-Electron Carbon Source. *Angew. Chem., Int. Ed.* **2015**, *54*, 951−955.
(32) Saran, R.; Stolojan, V.; Curry, R. J. Ultrahigh Performance C_{60} Nanorod Large Area Flexible Photoconductor Devices via Ultralow Organic and Inorganic Photodoping. *Sci. Rep.* **2014**, *4*, 5041.
(33) Chong, L. C.; Sloan, J.; Wagner, G.; Silva, S. R. P.; Curry, R. J. Controlled Growth of True Nanoscale Single Crystal Fullerites for Device Applications. *J. Mater. Chem.* **2008**, *18*, 3319−3324.
(34) Doi, T.; Koyama, K.; Chiba, Y.; Tsuji, H.; Ueno, M.; Chen, S.-R.; Aoki, N.; Bird, J. P.; Ochiai, Y. Electron Transport Properties in Photo and Supersonic Wave Irradiated C_{60} Fullerene Nano-Whisker Field-Effect Transistors. *Jpn. J. Appl. Phys.* **2010**, *49*, 04DN12.
(35) Takeya, H.; Miyazawa, K.; Kato, R.; Wakahara, T.; Ozaki, T.; Okazaki, H.; Yamaguchi, T.; Takano, Y. Superconducting Fullerene Nanowhiskers. *Molecules* **2012**, *17*, 4851−4859.
(36) Minato, J.; Miyazawa, K.; Suga, T. Morphology of C_{60} Nanotubes Fabricated by the Liquid−Liquid Interfacial Precipitation Method. *Sci. Technol. Adv. Mater.* **2005**, *6*, 272−277.
(37) Jin, Y. Z.; Curry, R. J.; Sloan, J.; Hatton, R. A.; Chong, L. C.; Blanchard, N.; Stolojan, V.; Kroto, H. W.; Silva, S. R. P. Structural and Optoelectronic Properties of C_{60} Rods Obtained via a Rapid Synthesis Route. *J. Mater. Chem.* **2006**, *16*, 3715−3720.
(38) Miyazawa, K. Synthesis of Fullerene Nanowhiskers using the Liquid−Liquid Interfacial Precipitation Method and Their Mechanical, Electrical and Superconducting Properties. *Sci. Technol. Adv. Mater.* **2015**, *16*, 013502.
(39) Okuda-Shimazaki, J.; Nudejima, S.; Takaku, S.; Kanehira, K.; Sonezaki, S.; Taniguchi, A. Effects of Fullerene Nanowhiskers on Cytotoxicity and Gene Expression. *Health* **2010**, *2*, 1456−1459.
(40) Nudejima, S.; Miyazawa, K.; Okuda-Shimazaki, J.; Taniguchi, A. Observation of Phagocytosis of Fullerene Nanowhiskers by PMA-Treated THP-1 Cells. *J. Phys.: Conf. Ser.* **2009**, *159*, 012008.
(41) Nudejima, S.; Miyazawa, K.; Okuda-Shimazaki, J.; Taniguchi, A. Biodegradation of C_{60} Fullerene Nanowhiskers by Macrophage-like Cells. In *Advances in Biomedical Research*; Anninos, P.; Rossi, M.; Pham, T. D.; Falugi, C.; Bussing, A.; Koukkou, M., Eds.; WAEAS Press: Athens, Greece, 2010, 89−94.
(42) Jensen, A. W.; Wilson, S. R.; Schuster, D. I. Biological Applications of Fullerenes. *Bioorg. Med. Chem.* **1996**, *4*, 767−779.
(43) Bakry, R.; Vallant, R. M.; Najam-Ul-Haq, M.; Rainer, M.; Szabo, Z.; Huck, C. W.; Bonn, G. K. Medicinal Applications of Fullerenes. *Int. J. Nanomed.* **2007**, *2*, 639−649.
(44) Bosi, S.; Da Ros, T.; Spalluto, G.; Prato, M. Fullerene Derivatives: an Attractive Tool for Biological Applications. *Eur. J. Med. Chem.* **2003**, *38*, 913−923.
(45) Bianco, A.; Kostarelos, K.; Prato, M. Applications of Carbon Nanotubes in Drug Delivery. *Curr. Opin. Chem. Biol.* **2005**, *9*, 674−679.
(46) Minami, K.; Kasuya, Y.; Yamazaki, T.; Ji, Q.; Nakanishi, W.; Hill, J. P.; Sakai, H.; Ariga, K. Highly Ordered 1D Fullerene Crystals for Concurrent Control of Macroscopic Cellular Orientation and Differentiation towards Large-Scale Tissue Engineering. *Adv. Mater. (Weinheim, Ger.)* **2015**, n/a.
(47) Shrestha, L. K.; Yamauchi, Y.; Hill, J. P.; Miyazawa, K.; Ariga, K. Fullerene Crystals with Bimodal Pore Architectures Consisting of Macropores and Mesopores. *J. Am. Chem. Soc.* **2013**, *135*, 586−589.
(48) Rasband, W. *ImageJ 1.44p*; National Institute of Health, Bethesda, MD, USA; http://imagej.nih.gov/ij (accessed Mar. 4, 2011).
(49) Shrestha, R. G.; Shrestha, L. K.; Khan, A. H.; Kumar, G. S.; Acharya, S.; Ariga, K. Demonstration of Ultrarapid Interfacial Formation of 1D Fullerene Nanorods with Photovoltaic Properties. *ACS Appl. Mater. Interfaces* **2014**, *6*, 15597−15603.
(50) Sathish, M.; Miyazawa, K. Synthesis and Characterization of Fullerene Nanowhiskers by Liquid-Liquid Interfacial Precipitation: Influence of C_{60} Solubility. *Molecules* **2012**, *17*, 3858−3865.
(51) Vidal, G.; Delord, B.; Neri, W.; Gounel, S.; Roubeau, O.; Bartholome, C.; Ly, I.; Poulin, P.; Labrugère, C.; Sellier, E.; et al. The Effect of Surface Energy, Adsorbed RGD Peptides and Fibronectin on the Attachment and Spreading of Cells on Multiwalled Carbon Nanotube Papers. *Carbon* **2011**, *49*, 2318−2333.
(52) Chung, T.-W.; Liu, D.-Z.; Wang, S.-Y.; Wang, S.-S. Enhancement of the Growth of Human Endothelial Cells by Surface Roughness at Nanometer Scale. *Biomaterials* **2003**, *24*, 4655−4661.
(53) Singh, A. V.; Ferri, M.; Tamplenizza, M.; Borghi, F.; Divitini, G.; Ducati, C.; Lenardi, C.; Piazzoni, C.; Merlini, M.; Podestà, A.; Milani, P. Bottom-Up Engineering of the Surface Roughness of Nanostructured Cubic Zirconia to Control Cell Adhesion. *Nanotechnology* **2012**, *23*, 475101.
(54) Teixeira, A. I.; Abrams, G. A.; Bertics, P. J.; Murphy, C. J.; Nealey, P. F. Epithelial Contact Guidance on Well-Defined Micro- and Nanostructured Substrates. *J. Cell Sci.* **2003**, *116*, 1881−1892.
(55) Curtis, A.; Wilkinson, C. Topographical Control of Cells. *Biomaterials* **1997**, *18*, 1573−1583.
(56) Badami, A. S.; Kreke, M. R.; Thompson, M. S.; Riffle, J. S.; Goldstein, A. S. Effect of Fiber Diameter on Spreading, Proliferation, and Differentiation of Osteoblastic Cells on Electrospun Poly(lactic acid) Substrates. *Biomaterials* **2006**, *27*, 596−606.
(57) Chew, S. Y.; Mi, R.; Hoke, A.; Leong, K. W. The Effect of the Alignment of Electrospun Fibrous Scaffolds on Schwann Cell Maturation. *Biomaterials* **2008**, *29*, 653−661.

DOI: 10.1021/acsami.5b04811
ACS Appl. Mater. Interfaces 2015, 7, 15667−15673